

REPORT DOCUMENTATION PAGE

Form Approved
OMB NO. 0704-0188

Public Reporting burden for this collection of information is estimated to average 1 hour per response, including the time for reviewing instructions, searching existing data sources, gathering and maintaining the data needed, and completing and reviewing the collection of information. Send comment regarding this burden estimates or any other aspect of this collection of information, including suggestions for reducing this burden, to Washington Headquarters Services, Directorate for information Operations and Reports, 1215 Jefferson Davis Highway, Suite 1204, Arlington, VA 22202-4302, and to the Office of Management and Budget, Paperwork Reduction Project (0704-0188,) Washington, DC 20503.

1. AGENCY USE ONLY (Leave Blank)	2. REPORT DATE	3. REPORT TYPE AND DATES COVERED <i>Reprint 8-18-03</i>
4. TITLE AND SUBTITLE Review of Dynamic Wake Models For Application to Dynamics and Stability of Rotorcraft		5. FUNDING NUMBERS GBUD #: 45667 Agreement #: DAAD19-01-1-0697
6. AUTHOR(S) David A. Peters		8. PERFORMING ORGANIZATION REPORT NUMBER None
7. PERFORMING ORGANIZATION NAME(S) AND ADDRESS(ES) Washington University, Box 1185 St. Louis, Missouri 63130-4899		
9. SPONSORING / MONITORING AGENCY NAME(S) AND ADDRESS(ES) U. S. Army Research Office P.O. Box 12211 Research Triangle Park, NC 27709-2211		10. SPONSORING / MONITORING AGENCY REPORT NUMBER <i>41304.9-EG</i>

11. SUPPLEMENTARY NOTES
The views, opinions and/or findings contained in this report are those of the author(s) and should not be construed as an official Department of the Army position, policy or decision, unless so designated by other documentation.

12 a. DISTRIBUTION / AVAILABILITY STATEMENT Approved for public release; distribution unlimited.	12 b. DISTRIBUTION CODE
--	-------------------------

13. ABSTRACT (Maximum 200 words)

See attached report

20030902 071

14. SUBJECT TERMS rotor wake model, induced flow, state space		15. NUMBER OF PAGES	
		16. PRICE CODE	
17. SECURITY CLASSIFICATION OR REPORT UNCLASSIFIED	18. SECURITY CLASSIFICATION ON THIS PAGE UNCLASSIFIED	19. SECURITY CLASSIFICATION OF ABSTRACT UNCLASSIFIED	20. LIMITATION OF ABSTRACT UL

**Review of Dynamic Wake Models
For Application to Dynamics and Stability
Of Rotorcraft**

David A. Peters
McDonnell Douglas Professor
Chairman, Mechanical Engineering
Washington University
Campus Box 1185
St. Louis, MO 63130

Proceedings of the 4th Australian Pacific Vertiflite Conference
On Helicopter Technology

Melbourne, Australia
July 21-23, 2003

This work was sponsored by the U.S. Army Research Office,
Agreement #DAAD19-01-1-0697, Tom Doligalski, Technical Monitor

REVIEW OF DYNAMIC WAKE MODELS FOR APPLICATION TO DYNAMICS AND STABILITY OF ROTORCRAFT

David A. Peters
McDonnell Douglas Professor
Chairman, Mechanical Engineering
Washington University
St. Louis, MO 63130

ABSTRACT

Since the introduction of dynamic inflow in the early 1970's, a fair amount of attention has been given to rotor induced flow models that are hierarchical and can be presented in state-space form. The original, heuristic, 3-state models of the 1970's gave way to the Pitt-Peters models of the 1980's that were hierarchical and could have as many as 8 states. In the late 1980's and early 1990's, the Peters-He models became completely hierarchical with as many states as desired. In more recent years, the emphasis has been on amending the model to include curved wakes, ground effect, and previously neglected states. Part of this development has necessarily involved computation of flow off of the rotor disk by the state-space approach. This paper reviews the developments up until now.

NOMENCLATURE

A	on-disk region	X	$\tan^{-1}(x/2)$
\hat{a}_n^m, \hat{b}_n^m	state variable	$\bar{\nabla}$	Laplace operator, non-dimensional
B	off-disk region	\bar{v}	nondimensional velocity, \bar{v}/V_∞
C	region of infinity	$v, \eta, \bar{\psi}$	ellipsoidal coordinates
D^c	damping matrix	Ψ	velocity potentials
H_n^m	combinatorial, Eq. (28)	Φ	pressure potentials
j	index	Λ	comparison functions
K_n^m	combinatorial, Eq. (27)	ξ	stream-line coordinate
L^c, \hat{L}^c	influence coefficients	ρ	density of air, kg/m^3
m	index	σ_n^m, ζ_n^m	coefficients, Eqs. (25-26)
M^c	mass matrix	τ	nondimensional time, $V_\infty t/R$
n	index	τ_n^m	pressure expansion coefficients
\bar{n}	normal vector	X	wake skew angle
P	pressure/ ρV_∞^2	ω	reduced frequency, $[\exp(i\omega\tau)]$
r	index	$()_0$	$m+n$ odd
R	disk radius, m	$()_e$	$m+n$ even
s	area A+B	$()_{\text{upper}}$	above disk
S	area A+B+C	$()_{\text{lower}}$	below disk
t	time, sec	$()_{!!}$	double factorial, Eq. (29)
\bar{v}	velocity, m/sec		
V_∞	free-stream, m/sec		
x, y, z	cartesian coordinates		

INTRODUCTION

Motivation

Whenever a rotorcraft manufacturer wishes to increase the performance, affordability, reliability, maintainability, or maneuverability of one of its aircraft, certain steps must always be followed whether the aircraft is entirely new or whether the aircraft is only to be modified. In particular, someone must have an idea (based on science and engineering) of what might be done to the aircraft to effect the required improvement. Second, one must determine how to model the change to the aircraft mathematically and numerically. Third, one must run an evaluation or simulation of the system (with and without the proposed changes) to determine the effectiveness of the proposed changes and the technical risks involved. This implies that, sooner or later, either a comprehensive rotorcraft code, a specialized rotorcraft code, or some type of flight simulation must be used to assemble the new technology (along with the rest of the aircraft) and to test the utility of the new concept through off-line computations or real-time simulations. Typically, such calculations and simulations must be made repeatedly in a design environment in order to test the myriad of possibilities and to come either to an optimum design or to the conclusion that the proposed system does not do what it was intended to do. This is at the heart of rotorcraft systems design.

It follows that the various pieces of physics used in such preliminary design and flight simulation settings must be very efficient. For computations, they must be efficient enough to allow multiple cases to be run; and, for flight simulation, they must be able to run in real time. On the other hand, the physics must be detailed enough to capture the important phenomenological response and to give realistic estimates of performance. Nowhere is this more true than in the modeling of the rotor wake. The rotor wake is one of the most important pieces of physics for performance, loads, stability, handling qualities, and

maneuvering of a rotorcraft. Yet the wake is so complex that attempts to model it by CFD or by vortex lattice methods become too complicated to be used in repetitive dynamics and handling qualities applications or in real time simulation.

The need for wake modeling that can be efficient enough to be applied in real-time flight simulation, in conventional stability and control analyses, and in preliminary design studies has led to the development of inflow models based on states that represent inflow modes. These have developed over the past 50 years into powerful tools that are used routinely in rotorcraft analysis. Although these tools will never completely replace more computational methods, such as CFD and vortex lattice, they nevertheless have an important ecological niche in the competitive world of inflow methodologies.

Background

The history of dynamic wake modeling covers the last 55 years. In 1948, Ken Amer postulated that the wake responded dynamically to pilot pitch and roll commands, [1] but he had no mathematical model. Sissingh [2] developed a model from momentum considerations, but it was a cumbersome, quasi-steady theory. Carpenter and Fridovich discovered how to compute the time delay of the wake in 1953, but they treated only thrust and did not consider pitch or roll [3]. In 1957, Loewy developed an unsteady wake model for climb, but it was only in the frequency domain [4]. In 1964, Jones introduced an actuator-disk model of quasi-steady flow for edgewise flight [5]. This led to the more general work of Joglekar and Loewy [6]. In 1970, Pat Curtiss simplified the Sissingh approach, but it was still primarily a quasi-steady theory [7]. In 1972, Bob Ormiston had the idea for a three-state dynamic inflow model that would combine the momentum theory of Sissingh with the time delays of Carpenter and Fridovich. He and Dave Peters developed this concept into a full hover theory [8-9] from 1972-1974. The model reduced to the Curtiss results at zero frequency and gave excellent correlation with hover data

over the entire frequency range. Nevertheless, the model was inadequate for forward flight.

Pitt and Peters developed 3-state and 5-state models for forward flight from first principles [10-12] during 1980-1983. These reduced to the previous model in hover, but gave similarly good correlations in forward flight at all advance ratios and all frequencies. The model, however, was limited to only the crudest wake descriptors of uniform flow with two simple gradients. Thus, the model could not predict flow detail beyond that necessary for thrust, roll moment, and pitch moment.

Beginning in 1987, Peters and his students at Georgia Tech showed that the entire rotor induced flow distribution could be found from dynamic, finite-state equations in terms of inflow mode shapes [13-15]. The theory was derived from the potential flow equations with only a few, plausible assumptions. By 1991, the complete theory was in a compact, closed form that could be immediately used for applications [16]. One thing, however, which the theory could not do adequately was to compute the unsteady flow everywhere in the flow field. Attempts were made to do this, and they were satisfactory at zero frequency; but results showed that a second set of states was required to compute the flow off disk [17].

This was the state of dynamic wake models in the early 1990's. Several important developments followed that changed the course of dynamic wake modeling. First, there was an unusual anomaly in helicopter flight mechanics that, during a pitching maneuver, experimental flight-test data showed that rotorcraft rolled opposite to what the simulations predicted even with the new wake models. Rosen, Ref. [18], suggested that this might be due to the effect of wake curvature on induced flow during the maneuver.

Curtiss and coworkers investigated this and found that this curvature effect could explain part of the anomaly and that simple vortex and momentum considerations could capture the effect, Refs. [19-20]. Barocela, corroborated these findings in his work on wake distortion, Ref. [21], although some discrepancies were noted with the work of

Curtiss, Ref. [22]. Barocela showed that the effect of wake curvature could be incorporated into the dynamic wake model of Pitt and Peters by allowing the coefficient matrices to be functions of both the wake skew and the wake curvature. This was completed by Krothapalli, et. al in Ref. [23].

The work on wake curvature was extended to the He model in References [24-26] in which it was shown that the entire coefficient matrix (involving all harmonics) could be modified to account for wake curvature. Reference [27] demonstrated that the work of Curtiss could be considered a special case of this more general formulation, thus uniting all of the various formulations together.

Another area of work on dynamic wake came with the need for ground effect calculations. The original He theory had included a simple ground-effect correction, but it became clear that something more general was needed in order to accommodate moving ground planes, inclined ground planes, and partial ground planes. References [28-31] progressed through a series of developments in which the He inflow model was used to treat ground effect. In these various approaches, either an image rotor or a ground plane source rotor was used to simulate the ground in a quasi-steady manner. For these cases, a second actuator disk (for the image rotor or ground rotor) was used, and the induced flow from that rotor needed to be computed on the primary rotor. This was done numerically by an off-line quasi-steady approach.

From that work, it became clear that what was needed was a completely unsteady theory that could compute the induced flow of these secondary rotors above the disk plane and in all three components. The He model, however, was unable to do this; and, therefore, the need was established for a more general treatment of inflow dynamics. This led to an entirely new methodology for induced flow dynamics.

Reference [32] outlined an approach for deriving dynamic wake equations in terms of velocity potentials rather than merely normal velocity components at the rotor disk. Such a formulation was shown to be derivable from a

Galerkin procedure applied to the potential flow equations. In Reference [33], this methodology was successfully implemented. Reference [34] demonstrated that this method contained the old He model (and, consequently, the Pitt-Peters model) as a special case in which off-disk modes were neglected. References [35-36] demonstrated that the method did, indeed converge for all three components of flow in the entire half space including the plane of the rotor disk and the semi-sphere above it.

This new methodology offers the possibility of completely unsteady ground effect work. Once the wake curvature terms are added to the new formulation, it also gives a unified treatment of all effects thus far investigated. In the sections to follow, we will look at the development of the new theory and comparisons of results under various assumptions and conditions.

DEVELOPMENT

Fluid-Dynamics Equations

The three-dimensional potential flow equations (momentum and continuity equations) for the pressure and velocity fields P and \bar{v} , with a free-stream velocity V_∞ , are

$$\frac{\partial \bar{v}}{\partial \tau} - \frac{\partial \bar{v}}{\partial \xi} = -\bar{v}P \quad (1)$$

$$\bar{v} \cdot \bar{v} = 0 \quad (2)$$

These equations have been non-dimensionalized by defining P as pressure divided by ρV_∞^2 , \bar{v} as induced velocity divided by V_∞ , and time as a reduced time τ , (i.e., time multiplied by V_∞/R .) The variable ξ is the non-dimensional coordinate along the free-stream line, positive upstream. All lengths are divided by the rotor radius R . Figure 1 shows the coordinate system.

From continuity, Eq. (2), it is observed that \bar{v} can be expressed by a velocity potential that satisfies Laplace's equation. It can also be shown that P satisfies Laplace's equation. Therefore, P can be expressed as a summation of pressure potentials, Φ ; and \bar{v} can be

expressed as a summation of the gradient of velocity potentials, Ψ .

Pressure Potentials, and Velocity Potentials

To transform Eqs. (1) and (2) by a Galerkin method, it is required to expand the pressure potential, Φ , and the velocity potentials, Ψ , in terms of a complete set of functions, each of which satisfies Laplace's equation. In addition, they have to fulfill the boundary conditions for pressure in the case of Φ , and for velocity in the case of Ψ .

The boundary conditions for pressure are given by a discontinuity across the rotor disk. The use of an ellipsoidal coordinate system $[\nu, \eta, \bar{\psi}]$, has the advantage that any odd function in ν , will allow a representation of a discontinuity across the rotor disk. An additional advantage of using an ellipsoidal coordinate system is that an analytical solution of Laplace's equation is known and can be expressed as,

$$\Phi_n^{mc}(\nu, \eta, \bar{\psi}) = \bar{P}_n^m(\nu) \bar{Q}_n^m(i\eta) \cos(m\bar{\psi}) \quad (3)$$

$$\Phi_n^{ms}(\nu, \eta, \bar{\psi}) = \bar{P}_n^m(\nu) \bar{Q}_n^m(i\eta) \sin(m\bar{\psi}) \quad (4)$$

where $\bar{P}_n^m(\nu)$ and $\bar{Q}_n^m(i\eta)$ are normalized associated Legendre functions of first and second kind.

Since $\bar{P}_n^m(\nu)$ with $n+m$ odd is an odd function of ν as well as a function that satisfies Laplace's equation, it has a discontinuity across the disk. Therefore, Eqs. (3) and (4) can be used as the expansion functions for the pressure potentials. On the other hand, $\bar{P}_n^m(\nu)$ with $n+m$ even is an even function of ν , but its derivative with respect to z is an odd function of ν on the disk. Such functions can be used to represent mass sources at the rotor disk. Therefore, P can be written as a summation of terms that includes both pressure discontinuities and mass-sources terms. Additionally, it can be shown that the pressure potentials Φ_n^m result in velocity distributions with infinite kinetic energy. Therefore, these are not included in the pressure expansion.

$$P = - \sum_{m=0}^{\infty} \sum_{n=m+1}^{\infty} \left(\tau_n^{mc} \Phi_n^{mc} + \tau_n^{ms} \Phi_n^{ms} \right) \quad (5)$$

The boundary conditions for the velocity field are: (1) the velocity field far upstream from the rotor is equal to zero, and (2) there is a velocity discontinuity any place a vortex or vortex sheet exists in the flow field. These discontinuities only exist at the rotor blades and within the rotor wake.

If the velocity-field computational domain is limited to the infinite upper-half volume above the rotor disk (Fig.2) the functions to be used in the velocity expansion do not have to fulfill any discontinuity conditions. It is important to note that, in the case of perfectly edgewise flow, the wake is located on the rotor disk plane. Thus no convergence of this methodology is expected on the trailing region off the rotor disk for edgewise flow, since the assumption for the velocity potentials is no longer valid in this region.

In order to strongly satisfy the upstream boundary condition for the velocity field, the velocity potentials are defined as

$$\Psi_n^{mc} = \int_{\xi}^{\infty} \Phi_n^{mc} d\xi; \quad \Psi_n^{ms} = \int_{\xi}^{\infty} \Phi_n^{ms} d\xi$$

$$m = 0, 1, 2, \dots, \infty; \quad n = m, m+1, m+2, \dots, \infty \quad (6)$$

This strongly ensures a zero velocity upstream. As ξ approaches infinity, Ψ_n^m approaches zero. The velocity \bar{v} is taken as

$$\bar{v} = \sum_{m=0}^{\infty} \sum_{n=m}^{\infty} \left(\hat{a}_n^m \bar{\nabla} \Psi_n^{mc} + \hat{b}_n^m \bar{\nabla} \Psi_n^{ms} \right) \quad (7)$$

where Ψ_n^{mc} and Ψ_n^{ms} are defined by Eq. (6).

Substitution of Eqs. (5) and (7) into (1), and because \hat{a}_n^m , \hat{b}_n^m , τ_n^{mc} and τ_n^{ms} are functions of τ ; and Ψ_n^{mc} , Ψ_n^{ms} , Φ_n^{mc} , and Φ_n^{ms} are functions of the spatial coordinates, x , y , and z , Eq. (1) can be written for cosine terms as

$$\sum_{m=0}^{\infty} \sum_{n=m}^{\infty} \left(\bar{\nabla} \Psi_n^{mc} \frac{d\hat{a}_n^m}{d\tau} - \bar{\nabla} \frac{\partial \Psi_n^{mc}}{\partial \xi} \hat{a}_n^m \right) =$$

$$\sum_{m=0}^{\infty} \sum_{n=m+1}^{\infty} \bar{\nabla} \Phi_n^{mc} \tau_n^{mc} \quad (8)$$

Only the cosine terms are listed, since sine and cosine completely decouple. However, an

identical set of equations can be written for the sine terms.

Galerkin Approach

If a Galerkin approach is applied to solve the conservation of momentum equation, Eq. (8) is pre-multiplied by the gradient of each one of some test functions, Λ , integrated over the domain; and the integrals are set to zero. In a Galerkin methodology, the test functions are defined from the same set of functions used to expand the pressure potential, Φ , and the velocity potentials, Ψ ,

$$\Lambda_j^{rc} = \Phi_j^{rc}; \quad \Lambda_j^{rs} = \Phi_j^{rs}$$

$$r = 0, 1, 2, \dots, \infty; \quad j = r, r+1, r+2, \dots, \infty \quad (9)$$

When the Galerkin approach is applied, the conservation of momentum equation, Eq. (8), becomes

$$\iiint_V \bar{\nabla} \Lambda_j^{rc} \cdot \sum_{m=0}^{\infty} \sum_{n=m}^{\infty} \left(\bar{\nabla} \Psi_n^{mc} \frac{d\hat{a}_n^m}{d\tau} - \bar{\nabla} \frac{\partial \Psi_n^{mc}}{\partial \xi} \hat{a}_n^m \right) dV =$$

$$\iiint_V \bar{\nabla} \Lambda_j^{rc} \cdot \sum_{m=0}^{\infty} \sum_{n=m+1}^{\infty} \bar{\nabla} \Phi_n^{mc} \tau_n^{mc} dV$$

$$r = 0, 1, 2, \dots, \infty; \quad j = r, r+1, r+2, \dots, \infty \quad (10)$$

The Divergence Theorem allows volume integrals to be expressed as surface integrals, Fig. 2. Therefore, if this theorem is applied to Eq. (10), and because Λ_j^{rc} , Ψ_n^{mc} , and Φ_n^{mc} all fulfill Laplace's equation, Eq. (10) becomes

$$\sum_{m=0}^{\infty} \sum_{n=m}^{\infty} \iint_S \left(\Lambda_j^{rc} \frac{\partial \Psi_n^{mc}}{\partial \bar{n}} \frac{d\hat{a}_n^m}{d\tau} - \Lambda_j^{rc} \frac{\partial^2 \Psi_n^{mc}}{\partial \bar{n} \partial \xi} \hat{a}_n^m \right) dS =$$

$$\sum_{m=0}^{\infty} \sum_{n=m+1}^{\infty} \iint_S \Lambda_j^{rc} \frac{\partial \Phi_n^{mc}}{\partial \bar{n}} dS \tau_n^{mc}$$

$$r = 0, 1, 2, \dots, \infty; \quad j = r, r+1, r+2, \dots, \infty \quad (11)$$

or

$$\sum_{m=0}^{\infty} \sum_{n=m}^{\infty} \iint_S \left(\frac{\partial \Lambda_j^{rc}}{\partial \bar{n}} \Psi_n^{mc} \frac{d\hat{a}_n^m}{d\tau} - \frac{\partial \Lambda_j^{rc}}{\partial \bar{n}} \frac{\partial \Psi_n^{mc}}{\partial \xi} \hat{a}_n^m \right) dS =$$

$$\sum_{m=0}^{\infty} \sum_{n=m+1}^{\infty} \iint_S \frac{\partial \Lambda_j^{rc}}{\partial \bar{n}} \Phi_n^{mc} dS \tau_n^{mc}$$

$$r = 0, 1, 2, \dots, \infty; \quad j = r, r+1, r+2, \dots, \infty \quad (12)$$

where S represents the surface area of the upper-half inflow volume V , including the rotor disk plane, dS represents a differential area element; and \bar{n} is a unit-vector, outward normal

to dS . The surface S can be subdivided into three areas: two of them are located on the rotor disk plane ($z=0$), s , and correspond to the on-disk area, A , and the off-disk area, B ; and the third one corresponds to the area on the infinite dome, C (Fig.2). Therefore,

$$s = A + B; \quad S = s + C \quad (13)$$

The pressure potentials, Φ_n^{mc} , velocity potentials, Ψ_n^{mc} , and test functions, Λ_j^{rc} , are such that all the integrals over the dome surface, C , become zero. Therefore, the surface of integration becomes the rotor disk plane ($z=0$), s , and the normal outward vector is along the z axis. Therefore,

$$\frac{\partial}{\partial \bar{n}} = \frac{\partial}{\partial z} \quad (14)$$

If Eq. (14) is substituted into Eqs. (11) and (12), together with the definition of the velocity potentials and the test functions, Eqs. (6) and (9), they become

$$\sum_{m=0}^{\infty} \sum_{n=m}^{\infty} \iint_s \Phi_j^{rc} \left(\frac{\partial}{\partial z} \left(\int_0^{\infty} \Phi_n^{mc} d\xi \right) \frac{d\hat{a}_n^m}{d\tau} + \frac{\partial \Phi_n^{mc}}{\partial z} \hat{a}_n^m \right) ds = \sum_{m=0}^{\infty} \sum_{n=m+1}^{\infty} \iint_s \Phi_j^{rc} \frac{\partial \Phi_n^{mc}}{\partial z} d\tau_n^m \quad (15)$$

$$r = 0, 1, 2, \dots, \infty; \quad j = r, r+1, r+2, \dots, \infty$$

$$\sum_{m=0}^{\infty} \sum_{n=m}^{\infty} \iint_s \frac{\partial \Phi_j^{rc}}{\partial z} \left(\int_0^{\infty} \Phi_n^{mc} d\xi \frac{d\hat{a}_n^m}{d\tau} + \Phi_n^{mc} \hat{a}_n^m \right) ds = \sum_{m=0}^{\infty} \sum_{n=m+1}^{\infty} \iint_s \frac{\partial \Phi_j^{rc}}{\partial z} \Phi_n^{mc} d\tau_n^m \quad (16)$$

$$r = 0, 1, 2, \dots, \infty; \quad j = r, r+1, r+2, \dots, \infty$$

where ds is a differential area on $z=0$.

It should be noted that the terms with $m=n$ for Φ_n^m result in some infinite integrals. This is because the steady velocity field due to τ_n^m mass sources result in infinite kinetic energy as $\tau \rightarrow \infty$. Therefore, in this formulation, we cannot yet treat mass source terms for which $m=n$.

Equations (15) and (16) constitute two different forms of the momentum equation. Each one is a set of ordinary differential equations for the velocity potential coefficients in terms of the pressure coefficients. From Eqs. (15) and (16), it is observed that, for these sets of functions, the application of the Divergence Theorem allows one to move the derivative

with respect to the unit-outward normal direction, $\partial/\partial z$, from the velocity potentials, Ψ_n^{mc} (or from the pressure potentials, Φ_n^{mc}) to the test functions, Λ_j^{rc} . At this point, it is important to note that the Φ_n^m with $n+m$ odd are zero on the $z=0$ plane off the disk (B), whereas the z derivatives of Φ_n^m with $n+m$ even are zero on region B . Because of this, the Divergence theorem can be utilized with appropriate choice of $\partial/\partial z$ position such that all integrals are zero on region B . The result is a set of integrals that need only be evaluated on region A (on-disk) for which they can be evaluated in closed form. The expression obtained after applying this procedure can be condensed in the following equation.

$$[\tilde{L}^c] \{ \hat{a}_n^m \} + [D^c] \{ \hat{a}_n^m \} = [D^c] \{ \tau_n^{mc} \} \quad (17)$$

where $()^* = d()/d\tau$ and where each one of the elements of the \tilde{L}^c and D^c matrices are known in closed form. The expressions are shown in the Appendix.

Equation (17) is valid for any skew angle χ , which appears in the equation in the expressions for the wake influence coefficient matrix \tilde{L}^c . This equation can be further partitioned into two row-groups and two column-groups such that $m+n$ (or $j+r$) is odd and $m+n$ (or $j+r$) is even. These matrices are organized in the following way

$$\begin{bmatrix} [j+r=odd, \\ n+m=odd] & [j+r=odd, \\ n+m=even] \\ [j+r=even, \\ n+m=odd] & [j+r=even, \\ n+m=even] \end{bmatrix} \begin{Bmatrix} \{n+m=odd\} \\ \{n+m=even\} \end{Bmatrix} \quad (18)$$

If Eq. (17) is organized as suggested in Eq. (18), it can be partitioned as

$$\begin{bmatrix} [\tilde{L}]_{b,o} & [\tilde{L}]_{b,e} \\ [\tilde{L}]_{e,o} & [\tilde{L}]_{e,e} \end{bmatrix} \begin{Bmatrix} \{ \hat{a}_n^m \}_b \\ \{ \hat{a}_n^m \}_e \end{Bmatrix} + \begin{bmatrix} [D]_{b,o} & [D]_{b,e} \\ [D]_{e,o} & [D]_{e,e} \end{bmatrix} \begin{Bmatrix} \{ \tau_n^m \}_b \\ \{ \tau_n^m \}_e \end{Bmatrix} = \begin{bmatrix} [D]_{b,o} & [D]_{b,e} \\ [D]_{e,o} & [D]_{e,e} \end{bmatrix} \begin{Bmatrix} \{ \tau_n^m \}_b \\ \{ \tau_n^m \}_e \end{Bmatrix} \quad (19)$$

Potential Function Expansions

The non-dimensional pressure drop and mass flow added to the velocity field (both

across the disk), and the velocity everywhere in the upper-half plane can be computed for the cosine terms as

$$\frac{\Delta p}{\rho V_\infty^2} = [P_{lower} - P_{upper}]_{\eta=0} = 2 \sum_{m=0}^{\infty} \sum_{n=m+1, m+3, \dots}^{\infty} \bar{P}_n^m(\nu) (\tau_n^{mc})_o \cos(m\bar{\psi}) \quad (20)$$

$$\frac{\Delta \dot{m}}{\rho V_\infty} = [P_{lower} + P_{upper}]_{\eta=0} = 2 \sum_{m=0}^{\infty} \sum_{n=m+2, m+4, \dots}^{\infty} \bar{P}_n^m(\nu) (\tau_n^{mc})_e \cos(m\bar{\psi}) \quad (21)$$

$$\bar{v} = \sum_{m=0}^{\infty} \sum_{n=m}^{\infty} \hat{a}_n^m \bar{\nabla} \Psi_n^{mc} = \sum_{m=0}^{\infty} \sum_{n=m}^{\infty} \hat{a}_n^m \bar{\nabla} \left(\int_{\xi}^{\infty} \Phi_n^{mc} d\xi \right) \quad (22)$$

From Eq. (22), it is seen that, to compute the velocity field, it is required to compute the velocity potentials, Ψ_n^m , by a numerical integration

$$\Psi_n^m = \int_{\xi}^{\infty} \Phi_n^{mc} d\xi \quad (23)$$

To avoid numerical integration and in order to be able to express the velocity potentials in terms of potentials known everywhere in the flow field, a change of variable from \hat{a}_n^m to a_n^m is introduced

$$\left\{ \hat{a}_n^m \right\}^T \left\{ \Psi_n^{mc} \right\} = \left\{ a_n^{mc} \right\}^T \left\{ \sigma_n^m \Phi_{n+1}^{mc} + \zeta_n^m \Phi_{n-1}^{mc} \right\} \quad (24)$$

The constants σ_n^m and ζ_n^m are chosen such that the new velocity potential will give no singularities when gradients of it are taken.

$$\sigma_n^m = \frac{1}{K_n^m \sqrt{(2n+1)(2n+3)((n+1)^2 - m^2)}} \quad (25)$$

$$\zeta_n^m = \frac{1}{K_n^m \sqrt{(4n^2 - 1)(n^2 - m^2)}}; n \neq m \quad (26)$$

where

$$K_n^m = \left(\frac{\pi}{2} \right)^{(-1)^{n+m}} H_n^m \quad (27)$$

$$H_n^m = \frac{(n+m-1)!!(n-m-1)!!}{(n+m)!!(n-m)!!} \quad (28)$$

and

$$\begin{aligned} (n)!! &= (n)(n-2)(n-4)\dots(2), n = \text{even} \\ (n)!! &= (n)(n-2)(n-4)\dots(1), n = \text{odd} \\ (0)!! &= 1; (-1)!! = 1; (-2)!! = \infty; (-3)!! = -1 \end{aligned} \quad (29)$$

If a Galerkin approach is applied to Eq. (24), the following relationship can be obtained

$$\left\{ \hat{a}_n^m \right\} = \left[\tilde{L}^c \right]^{-1} \left[M^c \right] \left\{ a_n^m \right\} \quad (30)$$

where

$$\left[M^c \right] = \left[\tilde{L}^c \right]_{\chi=0} \quad (31)$$

and where $\left[\tilde{L}^c \right]$ is the same matrix as defined in Eq. (17) and in the Appendix.

Equation (24) can be used to express the velocity potentials in axial flow. [] If Eq. (24) is substituted into Eq. (22), it yields

$$v_z = \sum_{m=0}^{\infty} \sum_{n=m+1}^{\infty} a_n^m \bar{\nabla} \left(\sigma_n^m \Phi_{n+1}^{mc} + \zeta_n^m \Phi_{n-1}^{mc} \right) \quad (32)$$

Since

$$\frac{\partial \left(\sigma_n^m \Phi_{n+1}^{mc} + \zeta_n^m \Phi_{n-1}^{mc} \right)}{\partial z} = \Phi_n^m, n > m \quad (33)$$

the axial component of the velocity is given by

$$v_z = \sum_{m=0}^{\infty} \sum_{n=m+1}^{\infty} a_n^m \Phi_n^m \quad (34)$$

If Eq. (30) is substituted into Eq. (17), the set of ordinary differential equations for the velocity coefficients in terms of the pressure coefficients for skewed flow becomes,

$$\left[M^c \right] \left\{ a_n^m \right\} + \left[D^c \right] \left[\tilde{L}^c \right]^{-1} \left[M^c \right] \left\{ a_n^m \right\} = \left[D^c \right] \left\{ \tau_n^{mc} \right\} \quad (35)$$

In axial flow, this equation becomes,

$$\left[M^c \right] \left\{ a_n^m \right\} + \left[D^c \right] \left\{ a_n^m \right\} = \left[D^c \right] \left\{ \tau_n^{mc} \right\} \quad (36)$$

Thus, the equation presented in previous work for axial flow [32] is a particular case of Eq. (35) when $\chi = 0$.

RESULTS

In this section, we look at some of the results from the newest inflow methodology as compared with the older approach. We will consider results both in the frequency domain and in the time domain. In the frequency domain there are closed-form numerical expressions based on the convolution integral that can be used to compare the solutions with a known result. There are also closed-form solutions in the time domain to a step input.

With these, we can determine the accuracy and convergence properties of the methods.

Figure 3 shows results in the plane of the rotor disk, through the $y=0$ center-line both on the disk ($-1 < x < +1$) and up to one radial length off the disk ($-2 < x < +2$). The normal component of flow is plotted for an elliptical pressure distribution at zero frequency. The wake skew angle is zero, corresponding to purely axial flow as in hover or climb. The "exact" convolution result is compared with both the newer Galerkin approach and the older He model. For this case, all three results are identical. Only the real portion is present because of the zero frequency. Figure 4 shows the same results but at a reduced frequency of 2.3. Here, the new approach and the convolution have identical real and imaginary parts, but the older He model shows some error (of the order of 10%). This is the worst case for discrepancy between the old and new models. The difference is due to the coupling with off-disk inflow modes that are neglected in the He approach.

Figure 5 shows the same result, but for a cyclic pressure input and at a wake skew angle of 45° and zero frequency. Once again, the convolution approach, the He model, and the new model are identical. Figure 6 takes the same case but adds a reduced frequency of 4.0. Some error begins to show up in the new model downstream since convergence is slower for that case, and only ten shape functions are included in these results. The He method gives results only on the disk (not off); but it, too starts to deteriorate in accuracy toward the rear of the disk.

Figure 7 gives a more detailed examination of convergence with number of even terms added to the old He model. The graph gives an error norm (based on the square of velocity errors either on the rotor disk, $-1 < x < +1$, or off-disk, $-2 < x < +2$) for the normal component of velocity in axial flow. Ten terms are included in the old He shape functions ($n+m$ odd), and the number of new terms ($n+m$ even) is varied from zero to twelve. (Note, since terms come in alternating values of odd or even subscripts, there are half as many odd or

even terms as the number of the highest subscript.) One can see how the error quickly converges to zero both on disk and off disk. However, if too many even terms are added, numerical ill-conditioning can cause the error to climb back up. Therefore, an optimum approach is to take only $3/4$ as many even terms as there are odd terms.

Figure 8 demonstrates convergence for flow off the disk. The skew angle is a relatively steep 75° . Flow is plotted one rotor radius above the disk along the disk centerline both on and off of the disk. The normal component of velocity is computed for 10 odd and 10 even terms and also for the optimized 10 odd and only 7 even terms. One can see that there is improved convergence when fewer $m+n$ even terms are included than there are $m+n$ odd terms. The reason for this is that, while the $m+n$ odd terms (the old He theory) are very-well conditioned, the $m+n$ even terms are poorly conditioned. Thus, round-off errors build more rapidly in these new terms. Fortunately, the on-disk terms give a good on-disk result, so that only a few off-disk are needed. The optimum combination is about $1/2$ to $3/4$ as many even terms as odd. Then flow both on the disk and off the disk is satisfactory.

Similar results are obtained for the other two velocity components (azimuthal and radial), as shown in Fig. 9, which gives all three components of flow for a cyclic input at zero degrees skew angle. Peters-He results are only shown for the z component since that is the only component for which the model can produce results.

In addition to the above frequency domain results, correlations have also been done in the time domain. Figures 10 and 11 show results in the time domain for a step input in pressure. The normal component of flow is plotted for the case of axial flow and for a reduced time up to $t=7$. The exact solution is compared to the finite-state results with 10 even and 10 odd terms. Flow is plotted at the disk center, one-half radius out from the center and one radius out from the center. Virtually exact agreement is obtained. Figure 10 compares this result with that of the old Peters-He model at

the rotor center and at the rotor edge. The Peters-He model does very well for this case.

The Pitt-Peters and Peters-He models involve the wake skew angle in the equations of motion. The skew angle appears in the form of $X = \tan(\chi/2)$ where χ is the skew angle. Interestingly, in the coupling between the m -th and r -th harmonic, X appears only to the powers $(m+r)$ and $(m-r)$. It is envisioned that the wake curvature angle will appear in a similar way. However, since the wake curvature is small, only terms to the first power in κ are used. These have been determined to involve only the cross-coupling between the zeroth and first harmonics, and this has been done for the He model but not, as yet, for the newer Morillo model.

Conclusions and Recommendations

The development of the finite-state wake models has continuously left the previous theory as embedded within the new (as a special case). Results continue to correlate well with known solutions. Several things are left to complete the theory:

1. The forcing functions in the new theory presently do not include τ_0^0 , a uniform mass source. This will need to be added to complete what is necessary for ground effect work.
2. The wake curvature terms need to be determined for the new model.
3. Convergence of down-stream flow must be improved for the limit of edgewise flow.
4. A study needs to be done of the feasibility of computing inflow below the plane of the rotor disk and within the rotor wake.

Figures

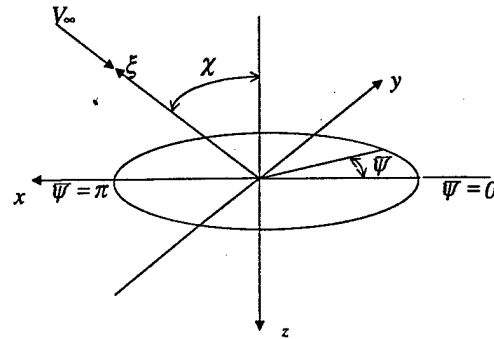


Fig.1 Coordinate system.

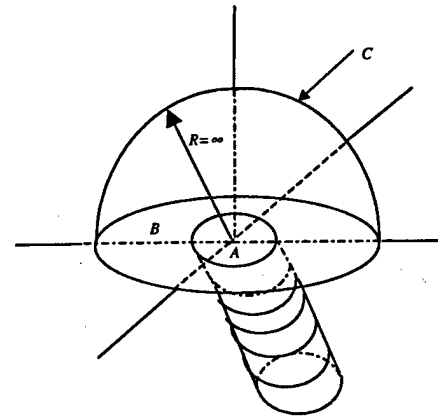


Fig.2 Volume and area of integration.

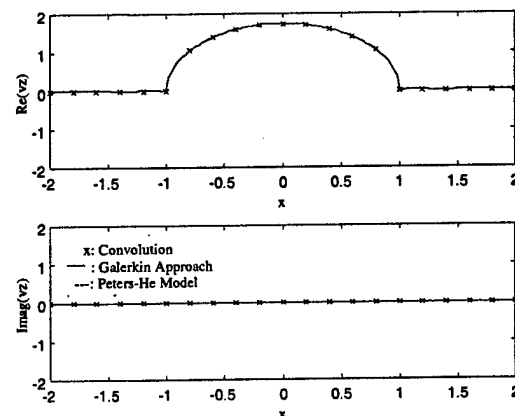


Fig. 3 Zero frequency response, $P = \Phi_1^0$, $\chi = 0^\circ$.

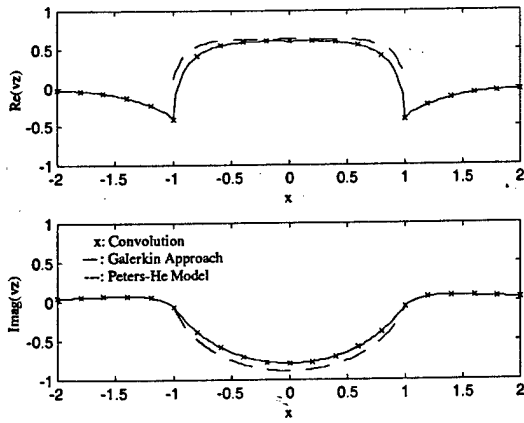


Fig. 4 Frequency response $\omega=2.3, P = \Phi_1^0, \chi=0^\circ$.

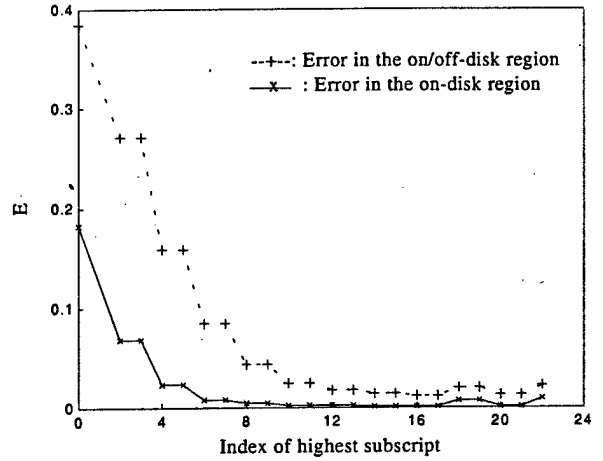


Fig. 7 Error, $\omega=2.3, P = \Phi_1^0, \chi=0^\circ, m_{odd}=20$.

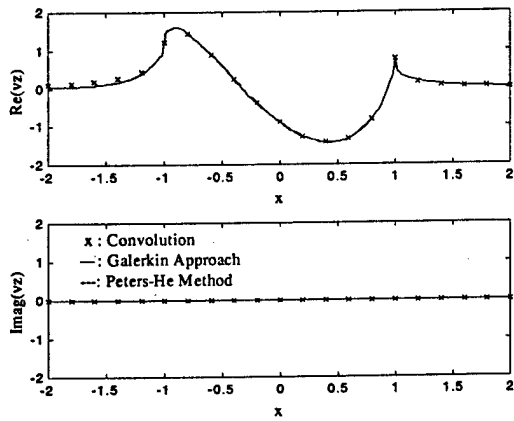


Fig. 5 Zero frequency response, $P = \Phi_2^1, \chi=45^\circ$.

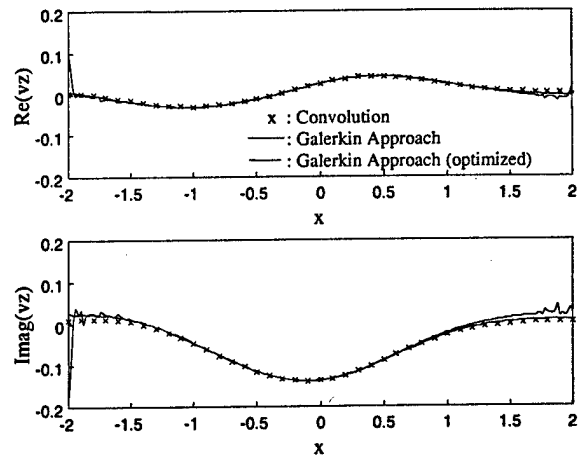


Fig. 8 Frequency response, $\omega=4.0, P = \Phi_1^0, \chi=75^\circ, z=-1$.

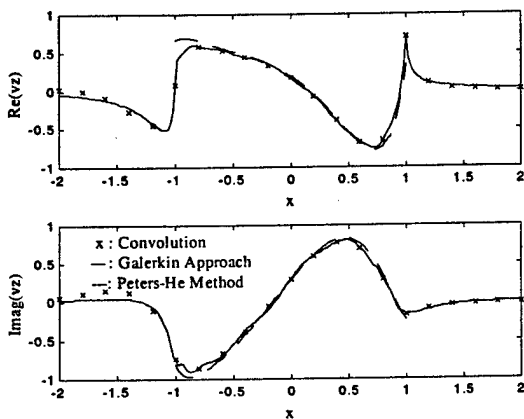
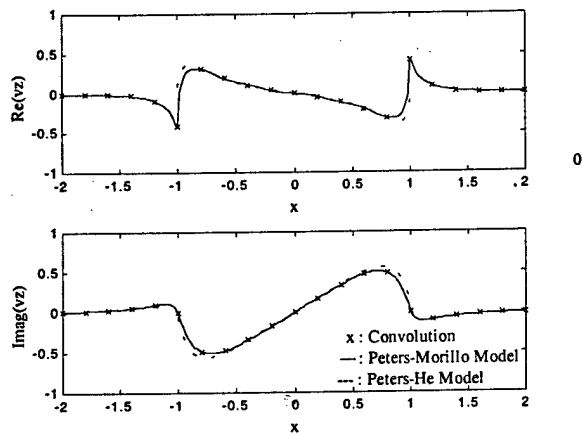
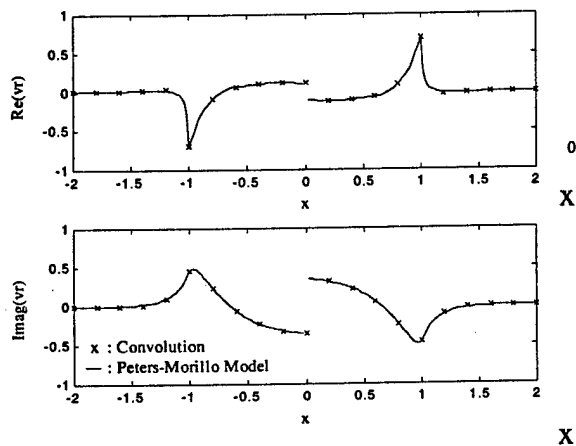


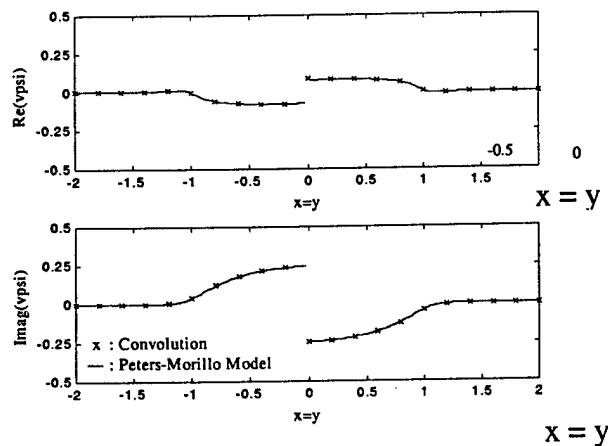
Fig. 6 Frequency response, $\omega=4, P = \Phi_2^1, \chi=45^\circ$.



(a)



(b)



(c)

Fig. 9 Frequency response $\omega=7.3$, $P = \Phi_2^1$, $\chi=0^\circ$.

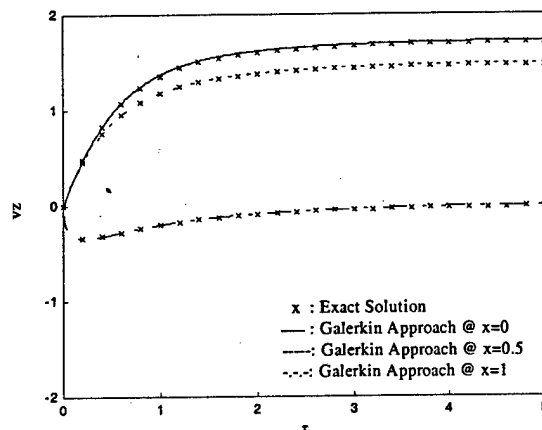


Fig. 10 Time response, $P = \Phi_1^0$, $\chi=0^\circ$, $z=0, y=0$.

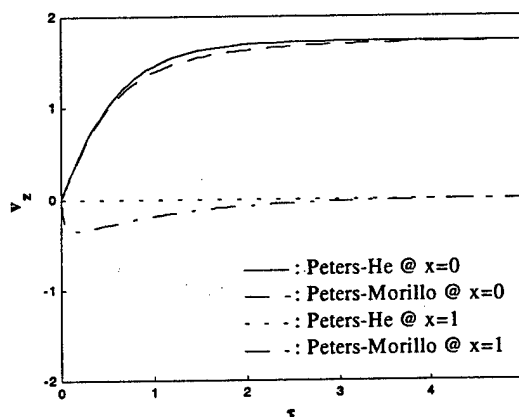


Fig. 11 Time response, $P = \Phi_1^0$, $\chi=0^\circ$, $z=0, y=0$.

REFERENCES

1. Amer, Kenneth B., "Theory of Helicopter Damping in Pitch or Roll and Comparison with Flight Measurements," NASA TN 2136, October 1948.
2. Sissingh, G.J., "The Effect of Induced Velocity Variation on Helicopter Rotor Damping in Pitch or Roll," A.R.C. Technical Report G.P. No. 101 (14,757, 1952.
3. Carpenter, P.J. and Fridovich, B., "Effect of a Rapid Blade Pitch Increase on the Thrust and Induced Velocity Response of a Full Scale Helicopter Rotor," NASA TN 3044, Nov., 1953.
4. Loewy, Robert G., "A Two Dimensional Approach to the Unsteady Aerodynamics of

- Rotary Wings," *Journal of the Aerospace Sciences*, Vol. 24, 1957, pp. 82-98.
5. Jones, J.P., "An Actuator Disc Theory for the Shed Wake at Low Tip Speed Ratios," MIT Aeroelasticity and Structures Laboratory Technical Report 133-1, 1965.
 6. Joglekar, M. and Loewy, R., "An Actuator-Disc Analysis of Helicopter Wake Geometry and the Corresponding Blade Response," USAAVLABS, Technical Report 69-66, 1970.
 7. Curtiss, Howard C., Jr., and Shupe, Norman K., "A Stability and Control Theory for Hingeless Rotors," Annual National Forum of the American Helicopter Society, Washington, D.C., May 1971.
 8. Ormiston, R.A., and Peters, D.A., "Hingeless Helicopter Rotor Response with Non-Uniform Inflow and Elastic Blade Bending," *Journal of Aircraft*, Vol. 9, No. 10, Oct. 1972, pp 34-39.
 9. Peters, D.A., "Hingeless Rotor Frequency Response with Unsteady Inflow," AHS/NASA Ames Specialists' Meeting on Rotorcraft Dynamics, NASA SP-362, February 1974.
 10. Pitt, Dale Marvin, *Rotor Dynamic Inflow Derivatives and Time Constants from Various Inflow Models*, Doctor of Science Thesis, Washington University, December 1980.
 11. Pitt, Dale M. and Peters, David A., "Theoretical Prediction of Dynamic-Inflow Derivatives," *Vertica*, Vol. 5, 1981, pp. 21-34.
 12. Pitt, Dale M. and Peters, David A., "Rotor Dynamic Inflow Derivatives and Time Constants from Various Inflow Models," Ninth European Rotorcraft Forum, Stresa, Italy, September 13-15, 1983, Paper No. 55.
 13. Peters, David A., Boyd, David Doug, and He, Cheng Jian, "A Finite-State Induce-Flow Model for Rotors in Hover and Forward Flight," *Journal of the American Helicopter Society*, Vol. 34, No. 4, October 1989, pp. 5-17.
 14. Peters, David A. and He, C-J, "Correlation of Measured Induced Velocities with a Finite-State Wake Model," *Journal of the American Helicopter Society*, Vol. 36, No. 3, July 1991, pp. 59-70.
 15. Su, Ay, Yoo, Kyung M., and Peters, David A., "Extension and Validation of an Unsteady Wake Model for Rotors," *Journal of Aircraft*, Vol. 29, No. 3, May-June, 1992, pp. 374-383.
 16. Peters David A. and Su, Ay, "An Integrated Airloads-Inflow Model for Use in Rotor Aeroelasticity and Control Analysis," 47 Annual Forum of the American Helicopter Society, Phoenix, May 6-8, 1991.
 17. Peters, David A. and Cao, Wenming, "Off-Rotor Induced Flow by a Finite-State Model," 37 AIAA SDM Conference, Salt Lake City, April 15-17, 1996, Paper 96-1550.
 18. Rosen, A. and Isser A., "A New Model of Rotor Dynamics During Pitch and Roll of a Helicopter," *Journal of the American Helicopter Society*, Vol. 40, (3), July, 1995.
 19. Keller, J.D. and Curtiss, H.C., Jr., "Modelling the Induced Velocity of a Maneuvering Helicopter," Proceedings of the American Helicopter Society 52nd Annual Forum, Washington, D.C., June 4-6, 1996, pp 841-851.
 20. Keller, J.D., "An Investigation of Helicopter Dynamic Coupling Using an Analytical Model," *Journal of the American Helicopter Society*. Vol. 41, (3), July 1995.
 21. Barocela, E., Peters, D.A., Krothapalli, K.R. and Prasad, J.V.R., "The Effect of Wake Distortion on Rotor Inflow Gradients and Off-Axis Coupling," AIAA paper 97-3559, 1997.
 22. Curtiss, H.C. Jr., "Aerodynamic Models and the Off-Axis Response," Proceedings of the American Helicopter Society 55th Annual Forum, Montreal, Canada, May 25-27, 1999.
 23. Krothapalli, K.R., Prasad, J.V.R., Peters, D.A., "Helicopter Rotor Dynamic Inflow Modeling for Maneuvering Flight," Proceedings of the 55th Annual National Forum of the AHS, The Society for Vertical Flight, Montreal, May 14-17, 1999, pp. 498-510.

24. Prasad, J.V.R., Zhao, J. and Peters, D.A., "Modeling of Rotor Dynamic Wake Distortion During Maneuvering Flight," Proceedings of the 2001 AIAA Atmosphere Flight Mechanics Conference, Montreal, Canada, 2002.
25. Zhao, J., Prasad, J.V.R. and Peters, D.A., "Rotor Dynamic Wake Distortion Model for Helicopter Maneuvering Flight." Presented at the 58th Annual Forum of the American Helicopter Society, Montreal, Canada, 2002.
26. Zhao, J., Prasad, J.V.R. and Peters, D.A., "Simplified Dynamic Wake Distortion Model for Helicopter Transitional Flight." presented at the AIAA Atmospheric Flight Mechanics Conference, Monterey, AIAA-2002-4400.
27. Prasad, J.V.R., Zhao, Jinggen, and Peters, David A. "Helicopter Rotor Wake Distortion Models for Maneuvering Flight," Proceedings of the 28th European Rotorcraft Forum, Bristol, UK, September 17-20, 2002, Pages 17.1-17.9.
28. Prasad, J. V. R., Xin, Hong, Peters, D. A., Nagashima, T. and Iboshi, N., "Development and Validation of a Finite State In-Ground Effect Inflow Model for Lifting Rotors," Proceedings of the AHS Technical Specialists' Meeting for Rotorcraft Acoustics and Aerodynamics, Stratford, Connecticut, October 28-30, 1997.
29. Xin, et al, "Ground Effect Aerodynamics of Lifting Rotors Hovering above Inclined Ground Plane," presented at the AIAA Applied Aerodynamics and CFD Conference, Norfolk, Virginia, June 28 - July 1, 1999, AIAA-99-3223.
30. Xin, Hong, Prasad, J. V. R., Peters, D. A., "Dynamic Inflow Modeling for Simulation of a Helicopter Operating in Ground Effect," presented at the AIAA Modeling and Simulation Technology Conference, Portland, Oregon, August 9 - 11, 1999, AIAA-99-4114.
31. Xin, H., Prasad, J. V. R., Peters, D., Ibushi, N. and Nagashima, T., "Correlation of Experimental Measurements with a Finite-State Ground Effect Model," Proceedings of the 56th Annual National Forum of the American Helicopter Society, Virginia Beach, May 1-4, 2000, pp. 421-430.
32. Peters, David A. and Morillo, Jorge A., "Towards a Complete Dynamic Wake Model in Axial Flow," Proceedings of the American Helicopter Society Aeromechanics Specialists' Meeting, Atlanta, Georgia, November 13-14, 2000.
33. Morillo, Jorge A. and Peters David A., "Extension of Dynamic Inflow Models to Include Mass Injection and Off-Disk Flow," Proceedings of the 40th AIAA Aerospace Sciences Meeting & Exhibit, Paper No. AIAA-2002-0716. Reno, Nevada, January 14-17, 2002.
34. Morillo, Jorge A., *A Fully Three-Dimensional Unsteady Rotor Inflow Model from a Galerkin Approach*, Doctor of Science Dissertation, Washington University, December 2001.
35. Morillo, Jorge A. and Peters, David A., "Convergence of a Complete Finite State Inflow Model of a Rotor Flow Field," Proceedings of the 28th European Rotorcraft Forum, Bristol, UK, September 17-20, 2002, Pages 66.1-66.10.
36. Morillo, Jorge A. and Peters, David A., "Velocity Field Above a Rotor Disk by a New Dynamic Inflow Model," *Journal of Aircraft*, Vol. 39, No. 3, September-October 2002.

ACKNOWLEDGEMENTS

This work was sponsored by the Georgia Tech/Washington University Center of Excellence in Rotary-Wing Technology, and funded by the National Rotorcraft Technology Center (Yung Yu, Technical Monitor). Funding also comes from the Boeing/Washington University Partnership (Ram Janakiram technical monitor), from NASA Ames (Chee Tung and Sam Crews technical monitors), and from the U.S. Army Research Office (Tom Doligalski technical monitor).